2023 8th International Conference on
Advanced Robotics and Mechatronics
July 8-10, Sanya, China

A Comparison of Hysteresis Models with the Hammerstein Structure for Piezoelectric Actuators

Yunzhi Zhang, Jie Ling, Zhao Feng and Yuchuan Zhu

Abstract— **Piezoelectric actuators (PEAs) can provide precision motion with fast response dynamics, large mechanical force, and high resolution. However, the strong hysteresis nonlinearity limits its application. In the last decades, lots of efforts on hysteresis cancellation have been made. Recent review articles have already described the progress of different hysteresis modeling and control approaches, but these articles focused mainly on the qualitative analysis of different models. This paper presents a comparison with both qualitative and quantitative analysis of these hysteresis models with the Hammerstein structure, including the differential-based models: a) Bouc-Wen (BW) and b) Asymmetrical BW (ABW) and the operator-based models: a) Prandtl-Ishlinskii (PI), b) PI with delay operators (DPI) and c) PI with polynomial (PPI). This paper presents an intuitive comparison of the characteristics of typical hysteresis models and detailed guidance to build a hysteresis model for the designers.**

I. Introduction

Piezoelectric actuators (PEAs) have been playing crucial roles in precision engineering due to the excellent advantages of fast response dynamics, large mechanical force, and high resolution. However, PEAs show strong hysteresis nonlinearity in practice, which affects the actuating accuracy [1], [2]. To improve the performance of PEAs, lots of efforts on hysteresis cancellation have been made, which can be roughly classified into two categories as: i) feedback control without hysteresis and ii) feedforward control with hysteresis model. Feedback control treats the nonlinearities as unmodelled dynamics or unknown disturbances [1]. Some modern control techniques such as repetitive control [3], damping control [4], [5] and sliding mode control [6], [7] are designed for PEAs in recent years. It succeeds in rejecting external disturbance, but the disadvantages of feedback control are also distinct, such as the negative influence of the sensor noise and disturbances to the entire system, the difficulty of the integration of the bulky sensors in such small systems like PEAs and so on [8], [9]. Therefore, feedforward control with the hysteresis model has been used as an alternative to achieve satisfactory results.

Feedforward control, control laws of which are derived based on the hysteresis models, has been developed to compensate for the hysteresis nonlinearities over the past decades. Thanks to the previous works of hysteresis modeling which are relatively mature, feedforward control of PEAs becomes more and more effective under different working conditions.

Conventional feedforward controller scheme is performed based on the inverse model [1], [2], [10]. This method is applied with two steps to design the feedforward controller. The first one is to build a precise hysteresis model characterizing the hysteresis behaviors. The second one is to obtain the corresponding inverse hysteresis model [2]. Despite the fact that this approach has been widely used with different kinds of hysteresis models, like Preisach model [11], [12], [13], [14], Prandtl-Ishlinskii (PI) model[15], [16], [17] and the modified versions of them [18], [19], [20], [21], the process of parameter identification and inversion calculation is always complex and challengeable. The inverse models are also sometimes inaccurate and fail to satisfy the constraint conditions. Moreover, it's proved to be hard to do inversion on some models like Bouc-Wen (BW) model [22], [23], [24], Krasnosel'skii–Pokrovkii (KP) model [25], [26], Maxwell model [27], [28] and Duhem model [29], [30], [31], which limits the validation of the approach [2].

In order to minimize the complexity of the above approach, some new methods based on the direct inverse hysteresis compensation concept [10] are developed. These methods directly utilize the available hysteresis models to describe the inverse hysteresis effect rather than modeling the hysteresis effect [9], [32], [33]. Without the process of building an inverse model, direct inverse hysteresis compensation meets the demand of more complicated modeling [34], [35], [36], [37]. Among them, the feedforward compensator with multiplicative-inverse structure (FFCMIS) is worth mentioning[8], [38], which is shown in Fig. 1. FFCMIS simplifies the feedforward compensation because it directly uses the hysteresis model for the compensator without any inversion calculation. Different hysteresis models own different forms of FFCMISs. There exist two FFCMISs which are respectively corresponding to the BW and PI. It should be noted that this method is only adaptive with static/ quasi-static conditions which are dependent on the feedforward controller design.

When it comes to rate-dependent hysteresis modeling, Hammerstein structure is a common approach. Cascading hysteresis nonlinearity with linear dynamics, the structure is proved effective to describe rate-dependent hysteresis [39], [40], [41]. In the system, the hysteresis nonlinearity is a static part that is available for the use of the FFCMIS.

*This work was supported by the Natural Science Foundation of Jiangsu Province (Grant No. BK20210294), the National Key Laboratory of Science and Technology on Helicopter Transmission (Grant No. HTL-A-22G03), and the Fundamental Research Funds for the Central Universities (Grant No. NS2022051).

Yunzhi Zhang, Jie Ling, and Yuchuan Zhu are with the College of Mechanical and Electrical Engineering, Nanjing University of Aeronautics and Astronautics, Nanjing 210016, China.

Zhao Feng is with the School of Power and Mechanical Engineering, Wuhan University, Wuhan 430072, China.

Corresponding author: Jie Ling, meejling@nuaa.edu.cn.

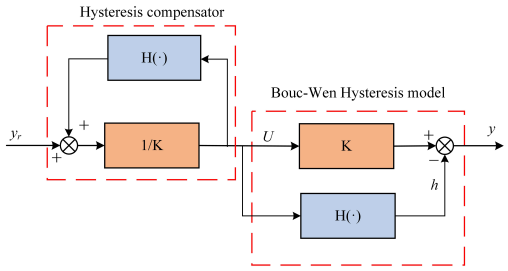

(a) BW with multiplicative-inverse structure

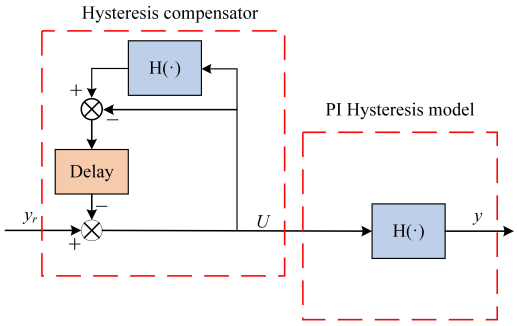

(b) PI with multiplicative-inverse structure

Fig. 1. multiplicative-inverse structure for PEAs (y_d denotes the desired command; u denotes the output of the designed controller; y denotes the actual reponse of the PEA).

However, in the previous literature, most of the FFCMISs are applied to the models directly describing the hysteresis, while the research on combining the Hammerstein structure with FFCMISs is limited so whether the FFCMIS is feasible to Hammerstein structure remains to be verified. Meanwhile, The comparison of several hysteresis models with the Hammerstein structure is also waiting to be done. Recent review articles have already described the progress of different hysteresis modeling and control approaches [1], [2], [10] for PEAs. But these articles focused mainly on the qualitative analysis of different models, including a) rate-dependent or not; b) difficulty in inversion calculation; c) Identification process. The quantitative analysis of hysteresis models with the Hammerstein structure owns the ability to intuitively analyze the characteristics of the models.

This paper is motivated to do the recurrence of Hammerstein structure with the several common hysteresis models, including the differential-based models: a) BW and b) Asymmetrical BW (ABW) and the operator-based models: a) PI, b) PI with delay operators (DPI) and c) PI with polynomial (PPI). On the basis of this, a comparison with both qualitative and quantitative analysis of these hysteresis models with the Hammerstein structure is made. This paper not only presents an intuitive comparison for the designers with the characteristics of typical hysteresis models, but also detailed guidance is provided to build the hysteresis models for a PEA.

II. Introduction of Hysteresis Models

A. Differential-based Models

Bouc-Wen model (BW) has been extensively applied in piezoelectric hysteresis modeling, the nonlinear part of which is a nonlinear differential equation form with a few parameters. Its mathematical expression is as follows [8]:

$$\begin{cases} y(t) = g(t) + h(t) \\ g(t) = kv(t) \end{cases} \tag{1}$$

$$\dot{h}(t) = \alpha\dot{v}(t) - \beta|\dot{v}(t)||h(t)|^n h(t) - \gamma\dot{v}(t)|h(t)|^n \tag{2}$$

where $g(t)$ and $h(t)$ are both the functions of input voltage $v(t)$, k is a linear gain and $y(t)$ denotes the output displacement. $\dot{h}(t)$ is the derivative of $h(t)$, $v(t)$ and $\dot{v}(t)$ are, respectively, the applied input excitation and its derivative with respect to time, and α, β, γ, n are the model parameters. The coefficient α controls the amplitude of the hysteresis loop, while β, γ control the shape of the hysteresis loop and n controls the smoothness of the transition from elastic to plastic response [42]. Because of the elastic structure and material of piezoelectric ceramics, n is generally admitted to describe the hysteresis of PEAs [44], [45], [46].

The BW model can only describe the symmetrical hysteresis loop which differs from the fact that the hysteresis loop will be asymmetrical in different working conditions in practice. Hence, the BW model is modified with an asymmetrical operator $\delta u(t) sign[\dot{u}(t)]$ [47], here the δ is the asymmetrical factor. The Asymmetrical BW model(ABW) is modified as follows:

$$\begin{aligned} \dot{h}(t) = {} & \alpha\dot{u}(t) - \beta|\dot{u}(t)|h(t)|^{n-1}h(t) - \gamma\dot{u}(t)|h(t)|^n \\ & + \delta u(t) sign[\dot{u}(t)] \end{aligned} \tag{3}$$

B. Operator-based Models

Prandtl-Ishlinskii model (PI) integrates a series of backlash operators H_r with different thresholds r, with different weights to describe the hysteresis nonlinear phenomenon of PEAs. When an input $u(t) \in C[0, T]$ which means $u(t)$ is a continuous function on the time interval $[0, T]$, is applied to PEAs, the output of the PI is given by the formula

$$Y[u](t) = w_0 u(t) + \sum_{i=1}^{n} w_i Hr_i[u](t) \tag{4}$$

$i = 1, 2, ..., n$, where n represents the number of backlash operators, w_i means the weights of each operator, and r_i are positive thresholds. Backlash operators H_r can be described in the following formula

$$Hr_i[u](t) = max(u(t) - r_i, min(u(t) + r_i, Hr_i[u](t - ts))) \tag{5}$$

ts means the sampling period. The fact that real actuator hysteretic loops sometimes are not symmetric is mentioned above, previous works [9], [48], [49] also modified the PI model into an asymmetric one. The first common approach is adding a polynomial operator $v(t)$ with only odd powers with the PI model, the polynomial operator is shown as follows:

$$v(t) = P[u](t) = c_1 u(t) + c_3 u^3(t) + \cdots + c_m u^m(t) \tag{6}$$

Here, $c_i(i = 1, 3, \cdots, 2k-1)$ are the constants to be identified, $m = 1, 3, 5, \cdots, 2k-1$ is the order of the polynomial. Previous works have mentioned that the 3-order polynomial operator is accurate enough to describe the asymmetric loop so that the modified PI model with polynomial operator is:

$$Y[u](t) = c_1 u(t)^3 + c_2 u(t) + \sum_{i=1}^{n} w_i H_{r_i}[u](t) \tag{7}$$

where c_1, c_2 are the weight parameters of the polynomial operator.

The second common approach is cascading the PI model with one-sided dead-zone operators (delay operators), the dead-zone operators $S_d[y](t)$ is shown as follows [49]:

$$S_d[y](t) = \begin{cases} \max\{y(t) - d, 0\}, & d > 0 \\ y(t), & d = 0 \end{cases} \tag{8}$$

d is the threshold of the one-sided dead-zone operator, $y(t)$ is the input of the operator. Then the output of one-sided dead-zone operators $z(t)$ can be given:

$$z(t) = \sum_{i=1}^{k} w_{s_k} S_{d_k}[y](t) \tag{9}$$

Here w_s is the weight of each one-sided dead-zone operator, and k is the number of one-sided dead-zone operators.

Based on the formula of the one-sided dead-zone operator, the modified PI model with one-sided dead-zone operators (DPI) can be given:

$$Y[u](t) = \sum_{k=1}^{m} w_{s_k} S_{d_k} \left\{ \sum_{i=1}^{n} w_i H_{r_i}[u](t) \right\} \tag{10}$$

Here w_s is the weight of each one-sided dead-zone operator, w is the weight of each backlash operator, k is the number of one-sided dead-zone operators, n is the number of backlash operators, and $Y[u](t)$ is the output of the DPI.

C. Hammerstein Structure

The Hammerstein structure shown in Fig. 2, cascades the static hysteresis nonlinearity with linear dynamics to model the rate-dependent hysteresis of PEAs. This structure divides

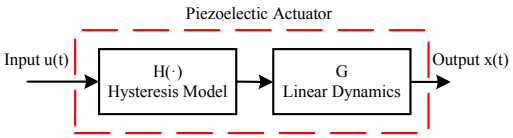

Fig. 2. Hammerstein structure

the model of PEAs into two parts. In practice, the part of linear dynamics is first gained through the step response of PEAs. On the basis of linear dynamics, the parameters of static hysteresis models can be identified with the data of the open-loop test.

III. Comparative Results of Different Hysteresis Models Under Low Input Voltage

In the following sections, the open-loop data are collected from a customized piezoelectric actuator [50]. The hysteresis models are built in the Matlab/Simulink environment, then comparisons are made through the experimental and simulation results.

A. Comparison of Differential-based Models with Hammerstein Structure

This paper first compares the modeling accuracy of differential-based models with the Hammerstein structure, including BW and ABW. The input signal is a sinusoidal signal of different frequencies (1-100Hz), and the amplitude of the voltage is 0-50v. Fig. 3 shows the comparison results of BW and ABW. The first and the second row (Fig. 3 (a-f)) are the simulation results of BW and ABW (1-50-100Hz). The third row (Fig. 3 (g-i)) shows the two models' errors. It should be mentioned first that the simulation data is recorded from the second half of the first period to the first part of the second period, which is the stable period of PEAs. Hence, the maximum output of PEAs (upper-right corner of the hysteresis loop) corresponds with the beginning and the end of the simulation data.

With Fig. 3, conclusions can be drawn that:

a) Both BW and ABW can simulate static hysteresis at 1Hz.

b) Neither BW nor ABW with Hammerstein structure can describe the rotation of the hysteresis loop, which is caused by the rate-dependent decrease of a maximum output of PEAs.

c) Simulation error of BW and ABW is extremely obvious at the maximum output of PEAs which increases with rate.

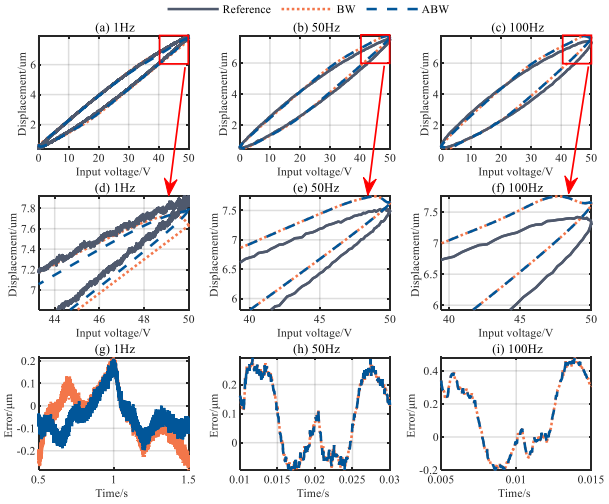

Fig. 3. Comparison of BW and ABW under 50V

B. Comparison of Operator-based Models with Hammerstein Structure

This paper then compares the modeling accuracy of operator-based models with the Hammerstein structure, in-

cluding the PI, DPI, and PPI. The conditions of the input signal are the same as before. As shown in Fig. 4, conclusions can be drawn that:

a) The PI, DPI, and PPI can simulate the static hysteresis at 1Hz.

b) The Hammerstein structure with the three models also failed to describe the rotation of the hysteresis loop.

c) Simulation errors of the PI, PPI, and DPI are extremely obvious at the maximum output of PEAs which increases with the rate.

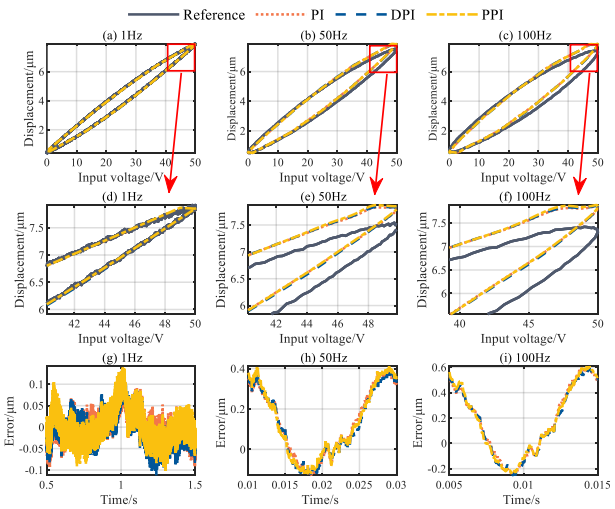

Fig. 4. Comparison of the PI, DPI, and PPI under 50V

Except for the three conclusions, it can also be observed that the operator-based models' accuracy is higher than the differential-based models' in static conditions. However, the difference in accuracy is eliminated with the negative influence of Hammerstein's structure. The accuracy of different hysteresis models is evaluated through the Root-mean-square error (RMSE) between the reference got from the open-loop test and the simulation, shown in Table I.

TABLE I

RMSE(μm) OF DIFFERENT HYSTERESIS MODELS

Hysteresis model	RMSE(1Hz)	RMSE(50Hz)	RMSE(100Hz)
BW	0.113	0.157	0.254
ABW	0.0923	0.157	0.254
PI	0.030	0.213	0.324
DPI	0.037	0.208	0.318
PPI	0.037	0.217	0.328

Hence, the Hammerstein structure has the disadvantage that it cannot simulate hysteresis rotation. Moreover, due to the rate-dependent property, hysteresis rotation becomes more obvious with the increase of the rate so that the modeling error becomes larger.

IV. Comparative Results of Different Hysteresis Models Under High Input Voltage

To further verify the accuracy evaluation of different models, the open-loop experiment of different working conditions under high input voltage is also conducted. The input signal is still the sinusoidal signal of different frequencies (1-100Hz), but the amplitude of the voltage is 0-140v. With the higher amplitude of input voltage, the PEAs will show the strong characteristics of asymmetry and saturation, which can be seen from Fig. 5. It should be mentioned that when the asymmetric hysteresis loop needs to be modeled, the asymmetric hysteresis model will take effect. The first row of Fig. 5 shows the PI while the second row shows the DPI and the third row is the error of the two models. Here, the RMS errors along with the NRMS errors within parentheses of the PI and DPI are calculated. At 1 Hz, 50 Hz and 100 Hz, the values of the PI are 0.76 μm (3.26%), 0.88 μm (3.34%) and 0.97 μm (3.97%) respectively. In contrast, the values of the DPI are 0.13 μm (0.54%), 0.52 μm (1.63%), 0.13μm (3.29%) and 0.68 μm (2.2%) respectively. Hence, it can be concluded that:

a) The PI fails to simulate the asymmetric hysteresis loop.

b) With the delay operators, the DPI can simulate the static asymmetric hysteresis loop at 1Hz.

c) The Hammerstein structure with the DPI fails to describe the rotation of the hysteresis loop. The simulation errors of the DPI are extremely obvious at the maximum output of PEAs which increases with the rate.

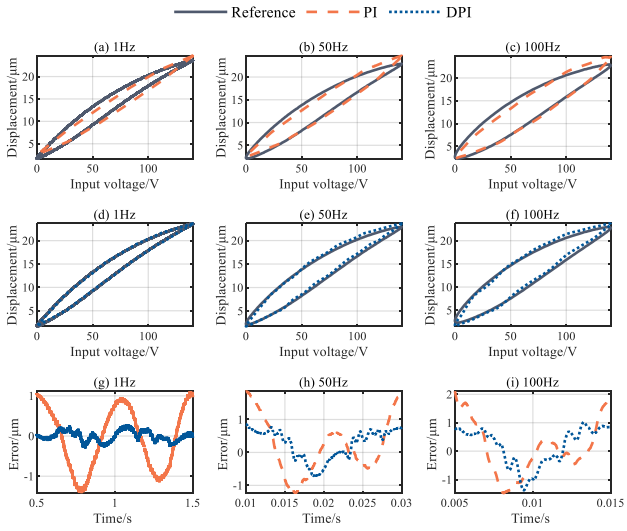

Fig. 5. Comparison of the PI and DPI under 140V

In addition, both the BW and ABW fail to describe the asymmetric hysteresis loop under 140V. The modeling results of the ABW can be seen in Fig. 6. The reason for the failure of ABW's validation is that: As shown in Fig. 6, the ascending curve of the asymmetric hysteresis loop is concave first and then convex. Even if ABW is a modified BW considering the asymmetry of the hysteresis loop, the ascending curves of ABW are always concave, which is different from the real asymmetric hysteresis loop.

To further explain the ABW's failure to simulate the asymmetric hysteresis loop under 140V, each parameter of ABW was studied through the control variate method. The

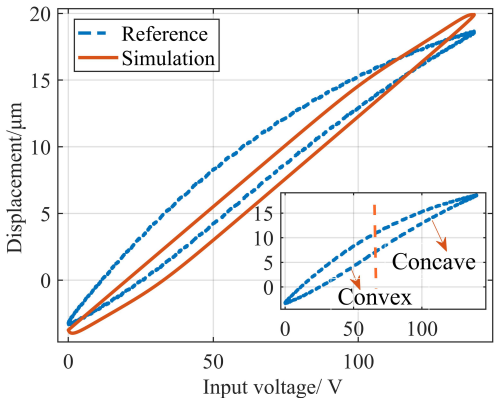

Fig. 6. ABW under 140V

initial parameter of [α, β, γ, δ] is [-0.3,0.0025,0.002,0.18]. The results are shown in Fig. 7. It can be concluded that:

a) If choose α as a variable, when it gradually increases, the amplitude of the hysteresis loop also increases, but the shape of the two vertices of the hysteresis loop does not change.

b) β and γ will change the shape of the hysteresis loop, but the simulated ascending curve keeps concave.

c) δ can describe the asymmetric properties of the loop, but it only changes the concavity and convexity of the descending curve.

V. CONCLUSIONS

This paper presents a comparison of hysteresis models with the Hammerstein structure with both qualitative and quantitative analysis, including the differential-based models: a) Bouc-Wen (BW) and b) Asymmetrical BW (ABW) and the operator-based models: a) Prandtl-Ishlinskii (PI), b) PI with delay operators (DPI) and c) PI with polynomial (PPI). The characteristics of the typical models under low input voltages and high input voltages are studied in depth based on a customized PEA platform. This paper presents an intuitive comparison of the characteristics of typical hysteresis models and detailed guidance to build a hysteresis model for the designers. It is found that most of the models with the Hammerstein structure can describe the asymmetric hysteresis precisely, however, the hysteresis rotation phenomenon especially in high frequency needs to be investigated further.

REFERENCES

[1] G. Gu, L. Zhu, C. Su, H. Ding, and S. Fatikow, "Modeling and control of piezo-actuated nanopositioning stages: A survey," *IEEE Transactions on Automation Science and Engineering*, vol. 13, no. 1, pp. 313–332, 2014.

[2] J. Gan and X. Zhang, "A review of nonlinear hysteresis modeling and control of piezoelectric actuators," *AIP Advances*, vol. 9, no. 4, p. 040702, 2019.

[3] Z. Feng, M. Ming, J. Ling, X. Xiao, Z. Yang, and F. Wan, "Fractional delay filter based repetitive control for precision tracking: Design and application to a piezoelectric nanopositioning stage," *Mechanical Systems and Signal Processing*, vol. 164, p. 108249, 2022.

[4] J. Ling, M. Rakotondrabe, Z. Feng, M. Ming, and X. Xiao, "A robust resonant controller for high-speed scanning of nanopositioners: Design and implementation," *IEEE Transactions on Control Systems Technology*, vol. 28, no. 3, pp. 1116–1123, 2019.

[5] J. Ling, Z. Feng, X. Kang, and X. Xiao, "Bandwidth enhancement in damping control for piezoelectric nanopositioning stages with load uncertainty: Design and implementation," *Journal of Vibration and Control*, vol. 27, no. 11-12, pp. 1382–1394, 2021.

[6] Z. Feng, W. Liang, J. Ling, X. Xiao, K. K. Tan, and T. H. Lee, "Integral terminal sliding-mode-based adaptive integral backstepping control for precision motion of a piezoelectric ultrasonic motor," *Mechanical Systems and Signal Processing*, vol. 144, p. 106856, 2020.

[7] J. Ling, Z. Feng, D. Zheng, J. Yang, H. Yu, and X. Xiao, "Robust adaptive motion tracking of piezoelectric actuated stages using online neural-network-based sliding mode control," *Mechanical Systems and Signal Processing*, vol. 150, p. 107235, 2021.

[8] M. Rakotondrabe, "Bouc–wen modeling and inverse multiplicative structure to compensate hysteresis nonlinearity in piezoelectric actuators," *IEEE Transactions on Automation Science and Engineering*, vol. 8, no. 2, pp. 428–431, 2010.

[9] Y. Qin, Y. Tian, D. Zhang, B. Shirinzadeh, and S. Fatikow, "A novel direct inverse modeling approach for hysteresis compensation of piezoelectric actuator in feedforward applications," *IEEE/ASME Transactions on Mechatronics*, vol. 18, no. 3, pp. 981–989, 2012.

[10] V. Hassani, T. Tjahjowidodo, and T. N. Do, "A survey on hysteresis modeling, identification and control," *Mechanical systems and signal processing*, vol. 49, no. 1-2, pp. 209–233, 2014.

[11] P. Ge and M. Jouaneh, "Tracking control of a piezoceramic actuator," *IEEE Transactions on Control Systems Technology*, vol. 4, no. 3, pp. 209–216, 1996.

[12] G. Song, J. Zhao, X. Zhou, and J. A. De Abreu-García, "Tracking control of a piezoceramic actuator with hysteresis compensation using inverse Preisach model," *IEEE/ASME Transactions on Mechatronics*, vol. 10, no. 2, pp. 198–209, 2005.

[13] C. Visone, "Hysteresis modeling and compensation for smart sensors and actuators," in *Journal of Physics: Conference Series*, vol. 138, no. 1. IOP Publishing, 2008, p.012028.

[14] R. V. Iyer and X. Tan, "Control of hysteretic systems through inverse compensation," *IEEE Control Systems Magazine*, vol. 29, no. 1, pp. 83–99, 2009.

[15] H. Janocha and K. Kuhnen, "Real-time compensation of hysteresis and creep in piezoelectric actuators," *Sensors and actuators A: Physical*, vol. 79, no. 2, pp. 83–89, 2000.

[16] P. Krejci and K. Kuhnen, "Inverse control of systems with hysteresis and creep," *IEE Proceedings-Control Theory and Applications*, vol. 148, no. 3, pp. 185–192, 2001.

[17] B. Mokaberi and A. A. Requicha, "Compensation of scanner creep and hysteresis for AFM nanomanipulation," *IEEE Transactions on Automation Science and Engineering*, vol. 5, no. 2, pp. 197–206, 2008.

[18] K. Kuhnen and P. Krejci, "Compensation of complex hysteresis and creep effects in piezoelectrically actuated systems—a new Preisach modeling approach," *IEEE Transactions on Automatic Control*, vol. 54, no. 3, pp. 537–550, 2009.

[19] G. Gu, L. Zhu, and C. Su, "Modeling and compensation of asymmetric hysteresis nonlinearity for piezoceramic actuators with a modified Prandtl–Ishlinskii model," *IEEE Transactions on Industrial Electronics*, vol. 61, no. 3, pp. 1583–1595, 2013.

[20] M. Al Janaideh, S. Rakheja, and C.-Y. Su, "An analytical generalized Prandtl–Ishlinskii model inversion for hysteresis compensation in micropositioning control," *IEEE/ASME Transactions on mechatronics*, vol. 16, no. 4, pp. 734–744, 2010.

[21] G. Gu, L. Zhu, and C. Su, "Integral resonant damping for high-bandwidth control of piezoceramic stack actuators with asymmetric hysteresis nonlinearity," *Mechatronics*, vol. 24, no. 4, pp. 367–375, 2014.

[22] M. Ismail, F. Ikhouane, and J. Rodellar, "The hysteresis Bouc-Wen model, a survey," *Archives of computational methods in engineering*, vol. 16, no. 2, pp. 161–188, 2009.

[23] P. Sengupta and B. Li, "Modified Bouc–Wen model for hysteresis behavior of RC beam–column joints with limited transverse reinforcement," *Engineering Structures*, vol. 46, pp. 392–406, 2013.

[24] D. Habineza, M. Rakotondrabe, and Y. Le Gorrec, "Multivariable generalized Bouc-Wen modeling, identification and feedforward control and its application to multi-DOF piezoelectric actuators," *IFAC Proceedings Volumes*, vol. 47, no. 3, pp. 10 952–10 958, 2014.

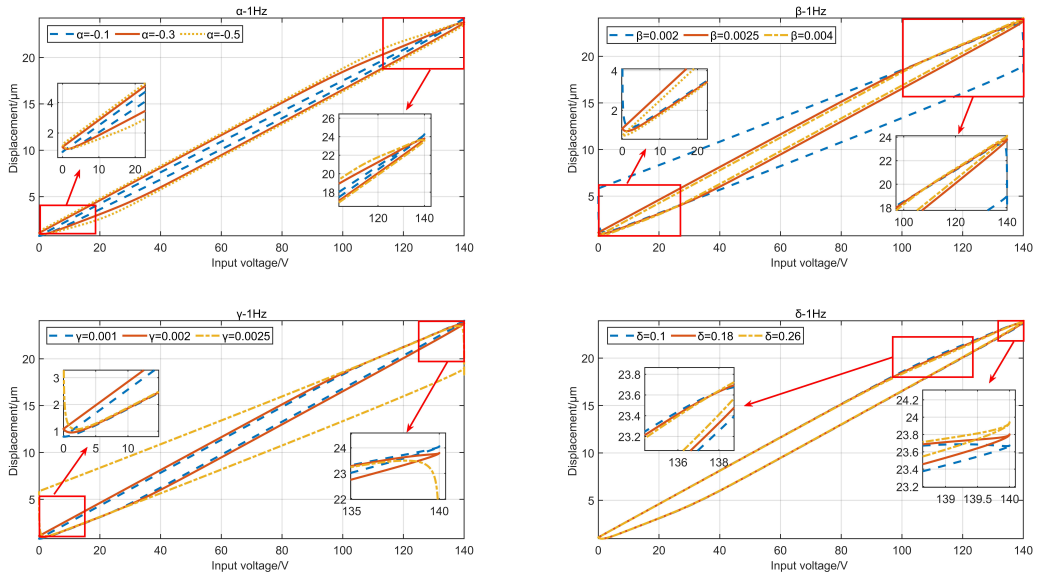

Fig. 7. Parameter evaluation of ABW under 140V

[25] G. V. Webb, D. C. Lagoudas, and A. J. Kurdila, "Hysteresis modeling of SMA actuators for control applications," *Journal of Intelligent Material Systems and Structures*, vol. 9, no. 6, pp. 432–448, 1998.

[26] W. S. Galinaitis, "Two methods for modeling scalar hysteresis and their use in controlling actuators with hysteresis," Ph.D. Dissertation, Virginia Tech, 1999.

[27] T. Tjahjowidodo, F. Al-Bender, H. Van Brussel, and W. Symens, "Friction characterization and compensation in electro-mechanical systems," *Journal of Sound and Vibration*, vol. 308, no. 3-5, pp. 632–646, 2007.

[28] M. Quant, H. Elizalde, A. Flores, R. Ramírez, P. Orta, and G. Song, "A comprehensive model for piezoceramic actuators: Modelling, validation and application," *Smart Materials and Structures*, vol. 18, no. 12, p. 125011, 2009.

[29] C. Lin and P. Lin, "Tracking control of a biaxial piezo-actuated positioning stage using generalized Duhem model," *Computers & Mathematics with Applications*, vol. 64, no. 5, pp. 766–787, 2012.

[30] A. K. Padthe, B. Drincic, J. Oh, D. D. Rizos, S. D. Fassois, and D. S. Bernstein, "Duhem modeling of friction-induced hysteresis," *IEEE Control Systems Magazine*, vol. 28, no. 5, pp. 90–107, 2008.

[31] B. D. Coleman and M. L. Hodgdon, "On a class of constitutive relations for ferromagnetic hysteresis," *Archive for Rational Mechanics and Analysis*, vol. 99, no. 4, pp. 375–396, 1987.

[32] M. Yang, C. Li, G. Gu, and L. Zhu, "Modeling and compensating the dynamic hysteresis of piezoelectric actuators via a modified rate-dependent Prandtl–Ishlinskii model," *Smart Materials and Structures*, vol. 24, no. 12, p. 125006, 2015.

[33] L. Cheng, W. Chen, and L. Tian, "A modified direct inverse Prandtl–Ishlinskii model based on two sets of operators for the piezoelectric actuator hysteresis compensation," *International Journal of Applied Electromagnetics and Mechanics*, vol. 68, no. 2, p. 177–191, 2022.

[34] T. Do, T. Tjahjowidodo, M. Lau, T. Yamamoto, and S. Phee, "Hysteresis modeling and position control of tendon-sheath mechanism in flexible endoscopic systems," *Mechatronics*, vol. 24, no. 1, pp. 12–22, 2014.

[35] T. Do, T. Tjahjowidodo, M. W. S. Lau, and S. J. Phee, "An investigation of friction-based tendon sheath model appropriate for control purposes," *Mechanical Systems and Signal Processing*, vol. 42, no. 1-2, pp. 97–114, 2014.

[36] Q. Xu and Y. Li, "Dahl model-based hysteresis compensation and precise positioning control of an XY parallel micromanipulator with piezoelectric actuation," *Journal of Dynamic Systems, Measurement, and Control*, vol. 132, no. 4, pp. 041011, 2010.

[37] Q. Xu and P.-K. Wong, "Hysteresis modeling and compensation of a piezostage using least squares support vector machines," *Mechatronics*, vol. 21, no. 7, pp. 1239–1251, 2011.

[38] M. Rakotondrabe, "Classical Prandtl-Ishlinskii modeling and inverse multiplicative structure to compensate hysteresis in piezoactuators," in *2012 American Control Conference (ACC)*. IEEE, 2012, pp. 1646–1651.

[39] X. Tan and J. S. Baras, "Modeling and control of hysteresis in magnetostrictive actuators," *Automatica*, vol. 40, no. 9, pp. 1469–1480, 2004.

[40] M. Al Janaideh, M. Rakotondrabe, I. Al-Darabsah, and O. Aljanaideh, "Internal model-based feedback control design for inversion-free feedforward rate-dependent hysteresis compensation of piezoelectric cantilever actuator," *Control Engineering Practice*, vol. 72, pp. 29–41, 2018.

[41] A. Cavallo, D. Davino, G. De Maria, C. Natale, S. Pirozzi, and C. Visone, "Hysteresis compensation of smart actuators under variable stress conditions," *Physica B: Condensed Matter*, vol. 403, no. 2–3, pp. 261–265, 2008.

[42] M. Ming, Z. Feng, J. Ling, and X. Xiao, "Hysteresis modelling and feedforward compensation of piezoelectric nanopositioning stage with a modified Bouc–Wen model," *Micro & Nano Letters*, vol. 13, no. 8, pp. 1170–1174, 2018.

[43] W. Zhu and X. Rui, "Hysteresis modeling and displacement control of piezoelectric actuators with the frequency-dependent behavior using a generalized Bouc–Wen model," *Precision Engineering*, vol. 43, pp. 299–307, 2016.

[44] T. Low and W. Guo, "Modeling of a three-layer piezoelectric bimorph beam with hysteresis," *Journal of Microelectromechanical Systems*, vol. 4, no. 4, pp. 230–237, 1995.

[45] Y. Li and Q. Xu, "Adaptive sliding mode control with perturbation estimation and PID sliding surface for motion tracking of a piezo-driven micromanipulator," *IEEE Transactions on Control Systems Technology*, vol. 18, no. 4, pp. 798–810, 2009.

[46] Q. Xu, "Identification and compensation of piezoelectric hysteresis without modeling hysteresis inverse," *IEEE Transactions on Industrial Electronics*, vol. 60, no. 9, pp. 3927–3937, 2012.

[47] W. Zhu and D. Wang, "Non-symmetrical Bouc–Wen model for piezoelectric ceramic actuators," *Sensors and Actuators A: Physical*, vol. 181, pp. 51–60, 2012.

[48] J. Gan and X. Zhang, "Modeling of rate-dependent hysteresis in piezoelectric actuators based on a modified Prandtl-Ishlinskii model," *International Journal of Applied Electromagnetics and Mechanics*, vol. 49, no. 4, pp. 557–565, 2015.

[49] W. T. Ang, P. K. Khosla, and C. N. Riviere, "Feedforward controller with inverse rate-dependent model for piezoelectric actuators in trajectory-tracking applications," *IEEE/ASME Transactions on Mechatronics*, vol. 12, no. 2, pp. 134–142, 2007.

[50] Y. Jiang and Y. Zhu, "Modeling and experimental study on radial dual-piezoelectric stack actuator," *Piezoelectrics & Acoustooptics*, vol. 43, no. 1, pp. 45–50, 2021.